

Busulfan Loading into Poly(alkyl cyanoacrylate) Nanoparticles: Physico-Chemistry and Molecular Modeling

Anne-Magali Layre,¹ Patrick Couvreur,¹ Hélène Chacun,¹ Caroline Aymes-Chodur,²
Nour-Eddine Ghermani,¹ Jacques Poupaert,³ Joël Richard,^{4*} Denis Requier,⁴ Ruxandra Gref¹

¹ UMR CNRS 8612, Faculty of Pharmacy, Paris-Sud University, Châtenay-Malabry, France

² EA 401, Faculty of Pharmacy, Paris-Sud University, Châtenay-Malabry, France

³ Medicinal Chemistry, School of Pharmacy, Université Catholique de Louvain, Brussels, Belgium

⁴ Ethypharm, Saint-Cloud, France

Received 7 October 2005; revised 16 November 2005; accepted 28 November 2005

Published online 21 August 2006 in Wiley InterScience (www.interscience.wiley.com). DOI: 10.1002/jbm.b.30536

Abstract: The busulfan is an alkylating agent widely used for the treatment of haematological malignancies and nonmalignant disorders. For a long time, it has been available only in an oral form. This treatment leads to a wide variability in bioavailability and side effects such as the veino-occlusive disease. Thus, an intravenous formulation of busulfan-loaded nanoparticles may be considered as a major progress. This study deals with busulfan entrapment by nanoprecipitation into five different types of poly(alkyl cyanoacrylate) polymers. The polymers leading to the highest busulfan loading efficiencies were poly(isobutyl cyanoacrylate) (PIBCA) and poly(ethyl cyanoacrylate). Molecular modeling along with energy minimization process was employed to identify the nature of the interactions occurring between busulfan and PIBCA. Further, optimization studies enabled to obtain PIBCA nanoparticles displaying busulfan loading ratios equal to 5.9% (w/w) together with nanoparticle yields of 71% (w/w). Since busulfan is a highly reactive molecule, we performed ¹H-NMR spectroscopy experiments showing that chemical integrity of the drug was preserved after loading into nanoparticles. The *in vitro* release studies under sink conditions, in water, or in rat plasma showed a fast release in the first 10 min followed by a slower one over 6 h. This phenomenon could be explained by the semi-polar characteristics of busulfan. © 2006 Wiley Periodicals, Inc. *J Biomed Mater Res Part B: Appl Biomater* 79B: 254–262, 2006

Keywords: computer modeling; drug delivery; nanotechnology; polymer

INTRODUCTION

A large number of pharmaceutical substances administered by the oral route are crystalline. In many cases polymorphism might cause several problems related to drug bioavailability and stability.¹ Efforts have been made towards the formulation of crystalline drugs to achieve preselected and desired properties.^{2,3} Because of their poor bioavailability, several crystalline drugs have to be administered by the intravenous route. Nanoparticles, small enough not to embolize the smallest capillary, have shown their ability to entrap and protect drugs.⁴ However, to our knowledge, only a few examples in the literature deal with the entrapment of crystalline drugs

within nanoparticles, and the entrapment efficiencies are always very poor.^{5–7}

The aim of this study was to assess the encapsulation of the strong crystalline busulfan drug into nanoparticles made by nanoprecipitation. Busulfan is a bifunctional alkylating agent, which interferes with DNA replication and transcription of RNA.⁸ It is widely used at a high dose as a part of a myeloablative regimen before both allogenic and autologous bone marrow transplantation, for the treatment of haematological malignancies⁹ and nonmalignant disorders such as immunodeficiency.¹⁰ For a long time, busulfan has been available only in an oral form, but a wide inpatient and outpatient variability in bioavailability in both adult and children has been reported.¹¹ Moreover, the veino-occlusive disease is a major side effect, which restricts the development of this molecule. This pathology has been correlated with a high systemic exposure to busulfan, expressed as the area under the plasma concentration–time curve.¹² Recently, there has been a main interest in developing an intravenous formulation of busulfan, which should be able to

Correspondence to: R. Gref (e-mail: ruxandra.gref@cep.u-psud.fr)

*Present address: Serono, Via di Valle Caia 22, 00040 Ardea (Roma), Italy

Contract grant sponsors: French National Research Center (CNRS)

Contract grant sponsor: Ethypharm

decrease the intrapatient and interpatient variability in bioavailability and to minimize the toxicity. Typical formulations were developed by dissolving busulfan in mixtures of organic solvent (*N,N*-dimethylacetamide or dimethylsulfoxide) and water.^{13,14} However, both organic solvents have their own well-documented toxicity also to be considered.^{15,16} To avoid the massive use of organic solvents, injectable colloidal carriers, such as liposomes¹⁷ and biodegradable polymer nanoparticles (polyesters¹⁸ and polyanhydrides¹⁹), have been developed. These carriers had, however, very low encapsulation efficiencies (0.4% (w/w) for liposomes and from 0.5 to 1.5% (w/w) for biodegradable polymer nanoparticles). These studies highlighted that busulfan encapsulation was very difficult to achieve, probably because of the strong crystalline character of this molecule. Indeed, the continuous leakage of this drug from the solid colloidal phase towards the liquid dispersion medium occurs during the nanoprecipitation process and never stops, because the drug spontaneously crystallizes in the dispersion medium, leading to the poor encapsulation efficiency observed. Thus, to encapsulate a crystalline drug with a high loading efficiency, the rationale is to use a polymer having a strong affinity for the drug, thus avoiding its leakage into the dispersion medium and its crystallization.¹⁹

In this study, we have investigated the loading of busulfan in five poly(alkyl cyanoacrylate) (PACA) polymers, using the nanoprecipitation process. Since busulfan has a high dipole moment,²⁰ it was suspected that there might be specific dipole–dipole interactions between busulfan and some PACA polymers. Thus, this study succeeded in efficiently encapsulating busulfan by choosing the best PACA polymer for the highest busulfan loading efficiency. For this composition, the formulation optimization, busulfan integrity in the nanoparticles, and *in vitro* release behavior were investigated.

MATERIALS AND METHODS

Materials

Alkyl cyanoacrylate monomers ethyl cyanoacrylate (ECA), propyl cyanoacrylate (PCA), butyl cyanoacrylate (BCA), isobutyl cyanoacrylate (IBCA), and isohexyl cyanoacrylate (IHCA) were kindly donated by Loctite (Ireland). Busulfan was purchased from Sigma-Aldrich, (France) and tritium-labeled busulfan from RC TRITEC (Switzerland). Poloxamer 188 (Synperonic PE/F68) was obtained from Fluka (France). Acetone was purchased from Carlo-Erba (France) and tetrahydrofuran (chromanorm) from VWR (France). Deuterated-acetone (acetone-d₆) and methanesulphonic acid (pure 99%) were supplied by Sigma-Aldrich (France). Rat plasma was obtained from Charles River (France).

Methods

Polymer Synthesis. The polymers were synthesized by anionic polymerization of alkyl cyanoacrylate monomers in water. The reaction scheme is described in Figure 1. The reaction was initiated by the attack of the hydroxyl groups present in

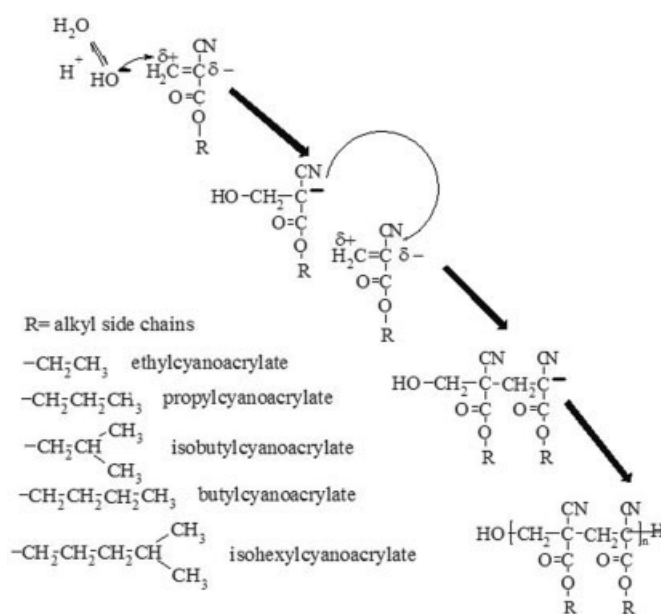


Figure 1. Reaction scheme of the anionic polymerization of alkyl cyanoacrylate monomers bearing different alkyl side chains (R).

water on the terminal methylene group of the alkyl cyanoacrylate monomers. The resulting carbanions behaved as nucleophiles and further reacted with other alkyl cyanoacrylate monomers to produce growing carbanion chains. This chain reaction resulted in the formation of PACA. Polymerization was stopped by mobile protons present in water. Practically, the monomer (1 mL) was added in one shot to water (15 mL). The polymerization was carried out for 1 h 30 at 40°C under magnetic stirring (1200 rpm). After this time, a milky suspension was obtained in the case of poly(butyl cyanoacrylate) (PBCA) and poly(isohexyl cyanoacrylate) (PIHCA). These polymers were collected by freeze-drying. In the case of poly(ethyl cyanoacrylate) (PECA), poly(isobutyl cyanoacrylate) (PIBCA), and poly(propyl cyanoacrylate) (PPCA), a milky suspension was obtained together with a polymer aggregate around the magnetic stirrer. These polymers were collected in two fractions. The milky suspension was freeze-dried. Separately, the aggregated polymer was dissolved in acetone and dried under vacuum at room temperature. The polymer thus obtained (representing more than 85% of the polymer synthesized) was used subsequently in the nanoprecipitation process.

Polymer Characterization. Polymer average number molar mass was determined by size exclusion chromatography (SEC; PL-GPC 220, Polymer Laboratories, UK) fitted with a refractive index detector (Polymer Laboratories). Laboratories PL Gel mixed B (Polymer Laboratories) and Shodex KF 802.5 (VWR) columns were set up in series. The features of the Laboratories PL Gel mixed B column were as given: molecular weights linear range stood between 500 and 10×10^6 g/mol (data given by the supplier); length, 300 mm; and internal diameter, 7.5 mm. The features of the Shodex KF 802.5 column were as given: molecular weight exclusion limit, 2×10^4 g/mol (data given by the supplier); length, 300 mm; and internal

diameter, 8 mm. Tetrahydrofuran at 35°C with a solvent flow of 1 mL/min was used as eluant. Polymers (5 mg) were dissolved in 5 mL of tetrahydrofuran and 200 μ L were injected into the chromatographic system. The polymer molar masses were determined with reference to a conventional calibration curve obtained using six polystyrene standards (Polymer Laboratories) having molar masses ranging from 580 to 3,114,000 g/mol.

The partition coefficient octanol–water (log P), which provides a thermodynamic measurement of the hydrophilic–lipophilic balance, was calculated using a computational method based on mathematical algorithms and structural information. Calculated log P (log K_{ow}) values were obtained using KowWin program (http://www.syres.com/esc/est_kowdemo.htm).

Nanoparticle Preparation. The nanoparticles were prepared by the nanoprecipitation process, as previously described by Fessi et al.²¹ Briefly, an organic solution of PACA (20 or 10 mg) and busulfan (2 mg) in acetone (1 mL) was injected into 2 mL water under magnetic stirring (1200 rpm) at room temperature, leading to spontaneous formation of nanoparticles. Acetone was removed using a rotative evaporator (Rotavapor®) at room temperature. The suspensions were purified by centrifugation (Jouan, MR22i) (5 min at 630 g), then by prefiltration (Acrodisc, Gelman Laboratory, Glass fiber membrane, 1 μ m), and finally by filtration (Millex®-HV, Millipore, 0.45 μ m) to eliminate drug crystals that might form during acetone evaporation step. All nanoparticles were treated this way, except the PBCA ones containing busulfan, which could not be filtrated. Drug-free nanoparticles were prepared according to the same procedure, without the purification steps.

Nanoparticle Size Determination. Nanoparticle mean diameters were measured using laser light scattering equipment (Coulter® N4MD, coulter Electronics, Margency, France). Each sample was properly diluted in water, so as to maintain the number of counts per second between 5×10^4 and 1×10^6 . Water was filtered with a 0.22 μ m filter to remove any impurities that could affect scattering of the light. Each sample was measured three times for at least 3 min at 20°C and at an angle of 90°. Both unimodal and size distribution processor analysis were performed. The stability of drug-free nanoparticles, maintained at 4°C, was studied.

Nanoparticle Drug Loading Determination. The drug loading of PACA nanoparticles was assessed using the tritium-labelled busulfan. ³H-Busulfan-loaded nanoparticles were prepared as described above, with a theoretical activity of 1.6 μ Ci/mg drug. The nanoparticles were collected by centrifugation (30,000g for 30 min) (Jouan, MR22i) and dried in a dessicator under vacuum at room temperature over 24 h. After weight determination, the nanoparticles were dissolved in 1 mL of acetone. The drug loading was determined by liquid scintillation counting. It was expressed as the amount of drug in nanoparticles divided by the weight of the nanoparticles collected [Eq. (1)].

$$\text{Drug loading} = \frac{(\text{amount of drug in nanoparticles})}{(\text{weight of nanoparticles})} \times 100 \quad (1)$$

The nanoprecipitation yield (NP Yield) was expressed as the weight of dried nanoparticles divided by the weight of polymers used in the nanoprecipitation procedure [Eq. (2)].

$$\text{NP yield} = \frac{(\text{dried weight of nanoparticles collected})}{(\text{weight of polymers initially introduced})} \times 100 \quad (2)$$

Molecular Modeling. The pentamer of isobutyl cyanoacrylate was initially drawn using ChemDraw in its syndiotactic stereochemistry and the model was converted to a 3D model using Chem3D 8.0. The model was energy-minimized using MM2 force field implemented in this package and the resulting structure was saved on a suitable input file that can be read in Hyperchem 7.0. This structure was again energy-minimized using first the Amber force field and then the semi-quantum method AM1 until the gradient value was inferior to 0.001 kcal/(mol Å). The Polak-Ribiere conjugate gradient method was used for all energy-minimization computations. Using the module of molecular dynamics (300 K, steps of 1 fsec) and the AM1 method, a trajectory of 250 psec was acquired and conformers were sampled every 5 psec. Heat and cool times were set to 0 psec and the bath relaxation time was set to 0.1 psec. The conformer having the lowest energy (heat of formation) was used to create a complex with busulfan. The initial model of busulfan was created in the same way as above and the resulting lowest energy conformer was finally energy-minimized by *ab initio* calculation at 6–31G* level. A complex of one busulfan molecule with one pentamer was assembled by disposing the molecules in a parallel way, and the same procedure of molecular dynamics and energy-minimization was repeated to generate the final models.

NMR Studies. Busulfan (5 mg), PIBCA polymer (10 mg), or drug-loaded nanoparticles (13 mg) were dissolved in acetone- d_6 (1 mL). The ¹H-NMR experiments were performed at 200 MHz using a Bruker ARX 200 MHz spectrometer. The measurements were performed at ambient temperature (300 K).

In Vitro Release Study. Drug release experiments were performed under “sink” condition at 37°C in water and in rat plasma. Freshly prepared tritium-labeled drug-loaded nanoparticle suspensions (theoretical activity of 5 μ Ci/mg busulfan) were diluted with the release medium studied. Then, nanoparticle suspension was separated in 1 mL aliquots and placed on a shaker (Heidolph, Titramax 101) at 37°C. At each given time-point, one aliquot was centrifuged (10 min at 30,000g). Busulfan in the supernatant was assessed by liquid scintillation counting. Nanoparticles were collected and dried in a dessicator for 24 h under vacuum at room temperature. After weight measurement, the nanoparticles were dissolved

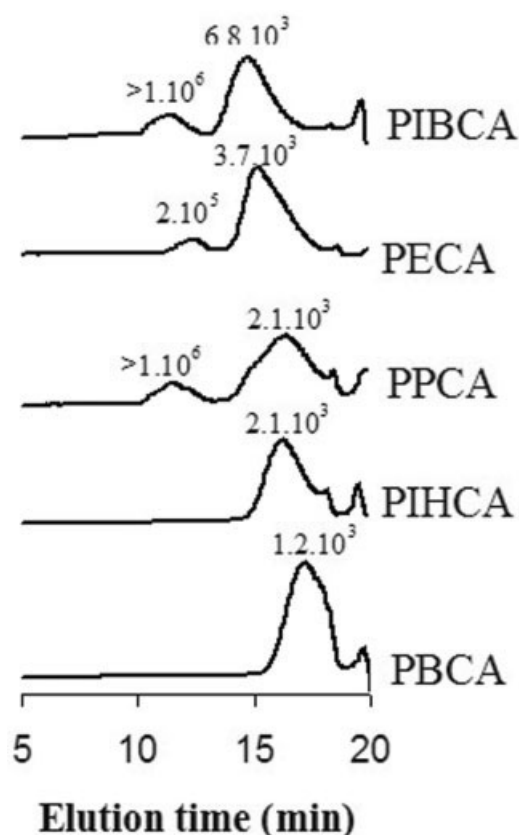


Figure 2. SEC chromatograms and calculated number-average molar masses (g/mol) of the synthesized PACA polymers.

in 1 mL acetone. The amount of busulfan remaining in the nanoparticle fraction was determined by liquid scintillation.

RESULTS AND DISCUSSION

Polymer Synthesis and SEC Analysis

SEC chromatograms and number-average molar masses (\bar{M}_n) are presented in Figure 2. Three of the PACA samples (PECA, PPCA, and PIBCA) showed a bimodal molar mass distribution, composed of a high molar mass fraction (2×10^5 g/mole or higher than 10^6 g/mol) and a lower molar mass fraction ($2.1\text{--}6.8 \times 10^3$ g/mol). The PBCA and the PIHCA polymers showed only one population of low molar mass ($1.2\text{--}2.1 \times 10^3$ g/mol), which corresponded to oligomers (7–11 units), as usually described in the literature.²² The differences in the molar mass distributions observed in Figure 2 could be interpreted on the basis of the different polymerization behavior of the monomers bearing alkyl chains with various lengths, as previously described.²³ It should be pointed out that with PBCA and PIHCA, a milky suspension was obtained after polymerization, whereas in the case of PECA, PPCA, and PIBCA, some aggregates were formed together with milky suspensions. The degree of polymerization, and therefore the molar mass, depends on a balance between initiation, propagation, and termination reactions.²⁴

In small-sized dispersed polymer particles, a high amount of terminating agent is available, so that polymerization is quickly stopped with the formation of oligomers.²² Contrarily, it is quite likely that in the large aggregates formed by PECA, PPCA, and PIBCA, there were not enough terminating agents available, and so the reaction was pursued until a high molar mass fraction was obtained. Indeed, further SEC chromatograms of the isolated milky suspensions showed only a single population of low molar mass species, the high molar mass one being absent (results not shown).

Drug-Free Nanoparticles

The nanoparticle mean diameter for all the PACA samples is summarized in Table I. The sizes of the nanoparticles prepared with or without Poloxamer 188 were not significantly different. The use of Poloxamer 188 at 0.1% (w/w) was not critical for nanoparticle formation, and this surfactant was not able to reduce the nanoparticle size. On the contrary, the mean diameter of drug-free nanoparticles strongly depended on the type of polymer used. PIBCA and PIHCA polymers lead to the smallest nanoparticles, with a size about 170 nm. The nanoparticle suspensions obtained with PECA and PPCA showed a mean diameter of about 210 nm, whereas the largest particles were obtained with PBCA (250 nm; Table I).

The calculated partition coefficients $\log K_{ow}$ of the different alkyl cyanoacrylate oligomers is summarized in Table II. It was observed that the $\log K_{ow}$ value of the different PACA depended both on the alkyl chain length and on the degree of polymerization n .

The polymers obtained with less lipophilic monomers (ECA and PCA) formed the nanoparticles with largest diameters (around 210 nm, Table I) whereas the polymers obtained with the most lipophilic monomers (PIBCA and PIHCA) lead to the smallest particles, with a size of 170 nm (Table I). PBCA was an exception to this rule. Indeed, PIBCA and PBCA had similar $\log K_{ow}$, although they had different molar mass distributions. This might be related to the fact that PBCA nanoparticles were larger than the PIBCA ones.

Figure 3 shows the stability of PECA, PPCA, and PIBCA nanoparticle suspensions incubated at 4°C. For all formulations, the mean diameter did not vary over 2 months. The presence of Poloxamer 188 (0.1% (w/w)) was not needed to

TABLE I. Z-Average Mean Diameters (nm) of Various PACA Nanoparticles

Polymer	Dispersing Medium	
	Water	Water + Poloxamer 188 (0.1% (w/v))
PECA	209 ± 47	194 ± 46
PPCA	218 ± 52	204 ± 59
PBCA	245 ± 46	241 ± 47
PIBCA	167 ± 38	170 ± 36
PIHCA	173 ± 36	180 ± 39

Values are the average of three different experiments ± SD.

TABLE II. Calculated Molar Masses (M_w), Log K_{ow} Parameters, and Increment of Log K_{ow} (Inc) for the Addition of One Monomer in the PACA Oligomers

Polymer	n	M_w (g/mol)	Log K_{ow}	Inc
PECA (n -C ₂ H ₅)	1	143	-1.031	
	2	268	-0.976	0.055
	3	393	-0.931	
PPCA (n -C ₃ H ₇)	1	157	-0.539	
	2	296	0.006	0.54
	3	435	0.552	
PIBCA (n -C ₄ H ₉)	1	171	-0.122	
	2	324	0.841	0.96
	3	477	1.804	
PBCA (n -C ₄ H ₉)	1	171	-0.049	
	2	324	0.988	1.04
	3	477	2.025	
PIHCA (n -C ₆ H ₁₃)	1	199	0.86	
	2	380	2.805	1.94
	3	561	4.75	

n , Number of monomers in the oligomer chain.

ensure this long-term stability. Similar data were obtained with PBCA and PIHCA (data not shown).

Busulfan Loaded Nanoparticles

Size and Drug Loading. As shown in Table III, the mean size of the busulfan nanoparticles was found to be quite similar to those of busulfan unloaded nanoparticles. All PACA nanoparticle suspensions showed a low nanoprecipitation yield, ranging from 6 to 33% (w/w), except the PBCA nanoparticle suspension (61% (w/w)).

Drug loading ranged from 0.5 to 6.2% (w/w), the best results being obtained with the PIBCA and PECA nanoparticles (Table III). As shown in Table III, drug loading increased as follows: PECA > PIBCA > PPCA > PIHCA > PBCA, whereas the alkyl chain length increased as follows: PIHCA > PIBCA > PBCA > PPCA > PECA. Therefore, no correlation could be found between the length of the monomer alkyl chains and the busulfan loading.

On the contrary, it was observed that busulfan loading increased with the PACA molar mass (Figure 2 and Table III). Possibly, the shorter polymer chains were able to organize in a more compact configuration than the longer ones, which have a lower degree of freedom. Sterical constraints into the matrix could lead, in the second case, to larger free volumes in the nanoparticles. Busulfan could be better fit inside these spaces, whereas it could be excluded from a dense matrix.

Formulation Optimization Using PIBCA. It clearly appears from Table III that PECA and PIBCA were the most effective in retaining busulfan into nanoparticles. Significant

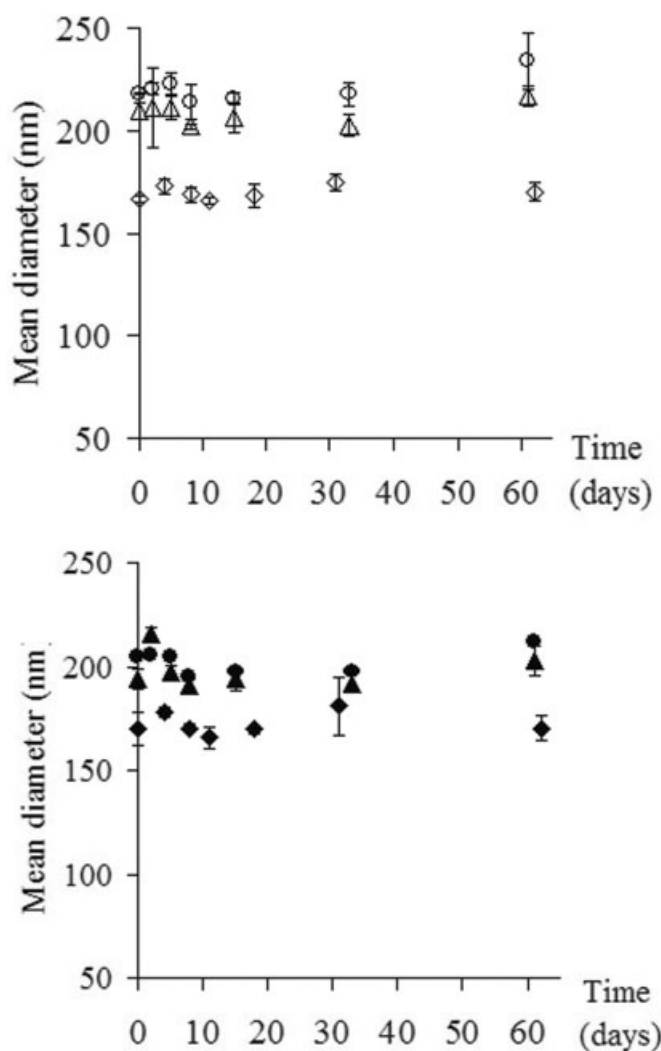


Figure 3. Stability of busulfan-free nanoparticles stored at 4°C in the absence (open symbols) or in the presence of Poloxamer 188 (0.1% (w/v)) (black symbols). Keys: Δ , PECA; \circ , PPCA; \diamond , PIBCA. Each value was the average of three different experiments \pm SD. For all preparations the polydispersity index was < 0.2.

amounts of this drug could thus be successfully entrapped in these PACA polymers, contrarily to polyesters that encapsulated only 1% (w/w) at the best.¹⁹ We therefore further

TABLE III. PACA Nanoparticle Features: Mean Diameter, Nanoprecipitation Yield, and Drug Loading Efficiency

Polymer	Polymer Concentration (mg/mL)	Mean Diameter (nm)	NP Yield (% w)	Drug Loading (% (w/w))
PECA	20	185 \pm 37	21 \pm 4	6.2 \pm 0.3
PPCA	20	180 \pm 56	6 \pm 2	3.8 \pm 0.5
PBCA	20	238 \pm 47	61 \pm 4	0.5 \pm 0.02
PIBCA	20	173 \pm 34	32 \pm 5	5 \pm 0.4
PIBCA	10	169 \pm 39	71 \pm 3	5.9 \pm 0.2
PIHCA	20	192 \pm 43	33 \pm 2	1.2 \pm 0.6

Values are the average of six different experiments \pm SD.

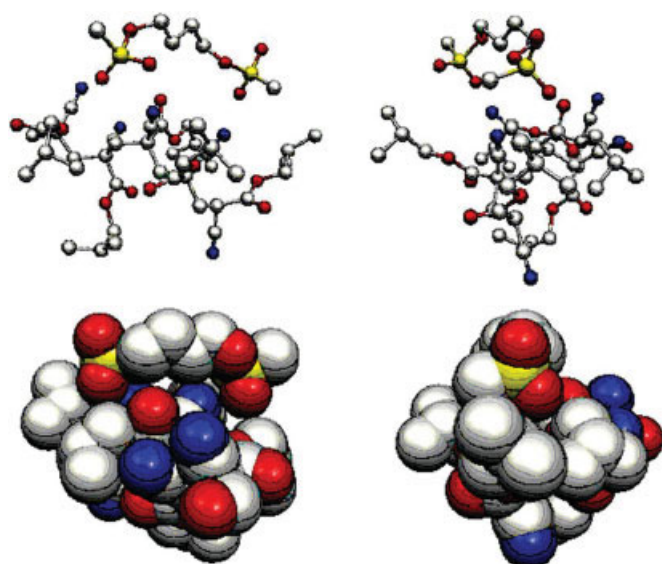


Figure 4. Two orientation views (in ball-and-stick (top) and space fill (bottom) modes) showing the results of the molecular modeling of the interaction between busulfan and one PIBCA pentamer. Carbon atoms are represented in grey, nitrogen atoms in blue, sulfur atoms in yellow, and oxygen atoms in red.

optimized the formulations using PIBCA, a polymer that showed a lower toxicity *in vitro* than PECA.^{25,26} Nanoparticles obtained by nanoprecipitation using PIBCA acetonitrile solution of 20 mg/mL had a mean diameter of 173 ± 34 nm (Table III). When the PIBCA concentration was decreased twice, the nanoparticle mean diameter was not significantly modified (169 ± 39 nm) and the busulfan loading slightly increased from (5 ± 0.4) to $(5.9 \pm 0.2)\%$ (w/w). However, the nanoprecipitation yield was strongly increased from (32 ± 5) to $(71 \pm 3)\%$ (w/w), when the PIBCA concentration decreased from 20 to 10 mg/mL. This could be related to a significant reduction of polymer aggregates during nanoprecipitation. We therefore choose a polymer concentration of 10 mg/mL in the next studies.

Molecular Modeling. The structure of the busulfan and one pentamer of PIBCA obtained after thermal equilibration for 250 psec at 300 K and AM1 minimization in vacuum is depicted in Figure 4. The molecule of busulfan displaying an extended conformation was found lying over the top of a folded polymer. Deeper inspection of the system revealed that the sulfur atoms of both methylsulfonate fragments of busulfan were in close interaction with the nitrogen atoms of the nitrile groups of the IBCA oligomer. Indeed, the smallest S...N interatomic distances were found equal to 3.503 and 3.580 Å, respectively. The corresponding approximate angles between C≡N and S—CH₃ bond directions of the nitrile and the methylsulfonate groups were found equal to 71.7° and 163.0° for the two pairs of interacting fragments, respectively. These findings support the hypothesis of charge-dipole and dipole-dipole interactions between the methylsulfonate fragments of busulfan and the nitrile groups of PIBCA.

This could also explain the high efficacy of PIBCA to encapsulate busulfan (Table III).

NMR Studies. NMR spectroscopy was used in complement to radioactivity studies to assess the busulfan loading into PIBCA nanoparticles and to study the integrity of the encapsulated drug. Indeed, busulfan is a very reactive compound, which readily degrades in water. The degradation of busulfan in aqueous solution has been already reported by several authors.^{27,28} The hydrolysis products were identified as tetrahydrofuran and methanesulphonic acid by ¹H-NMR.²⁸

¹H-NMR spectra of busulfan, PIBCA, busulfan-loaded nanoparticles, as well as of busulfan-loaded nanoparticles doped with tetrahydrofuran or methanesulphonic acid are presented in Figure 5. In agreement with previously published data,^{27,29,30} the busulfan spectra [Figure 5(a)] showed three resonance peaks at 1.7 (CH₂, multiplet), 2.9 (CH₃, singlet), and 4.1 ppm (CH₂; multiplet), and the PIBCA spectra [Figure 5(b)] showed four resonance peaks at 0.9 (CH₃, doublet), 1.9 (CH, multiplet), 2.5 (CH₂, multiplet), and 3.9 ppm (CH₂, multiplet). All the busulfan-loaded nanoparticle spectra contained the resonance peaks corresponding to PIBCA and busulfan [Figure 5(c)]. Moreover, these peaks appeared at the same chemical shifts as busulfan and PIBCA, indicating that there was no chemical reaction between PIBCA and busulfan.

¹H-NMR spectroscopy was further utilized to show that the busulfan entrapped in the nanoparticles was not degraded during the nanoprecipitation process. For this, the spectra of drug-loaded nanoparticles doped with small quantities of busulfan degradation products (tetrahydrofuran and methanesulphonic acid) were recorded [Figure 5(d)]. This spectrum showed three additional peaks compared to the NMR spectra of busulfan-loaded nanoparticles [Figure 5(c)]. These new peaks corresponded to the tetrahydrofuran resonance peaks at 3.5 (CH₂—O, multiplet) and 1.6 ppm (CH₂, multiplet) and to the methanesulphonic acid resonance peak at 2.8 ppm (CH₃, singlet). It was therefore concluded that busulfan was encapsulated in its native form and that none of its degradation products were present in the loaded PIBCA nanoparticles.

Moreover, it was possible to determine the busulfan loading in the PIBCA nanoparticles, using the peak areas obtained from ¹H-NMR analysis. Indeed, the peak B of busulfan at 4.1 ppm corresponded to the two protons of the CH₂—O functionality, and the peak F of IBCA at 3.9 ppm was attributed to the two protons of the CH₂—O functionality [Figure 5(c)].

Consequently, the weight of busulfan in the nanoparticles is given by $A_B/2 \times M_{Bu}$ and the weight of IBCA is given by $A_F/2 \times M_{IBCA}$.

Where A_B and A_F are the areas of the peak B and peak F, respectively (Table IV). Also, M_{Bu} and M_{IBCA} are the molar mass of busulfan (256 g/mol) and IBCA (153 g/mol), respectively.

Thus, the busulfan weight ratio into the nanoparticles may be calculated as follows [Eq (3)]:

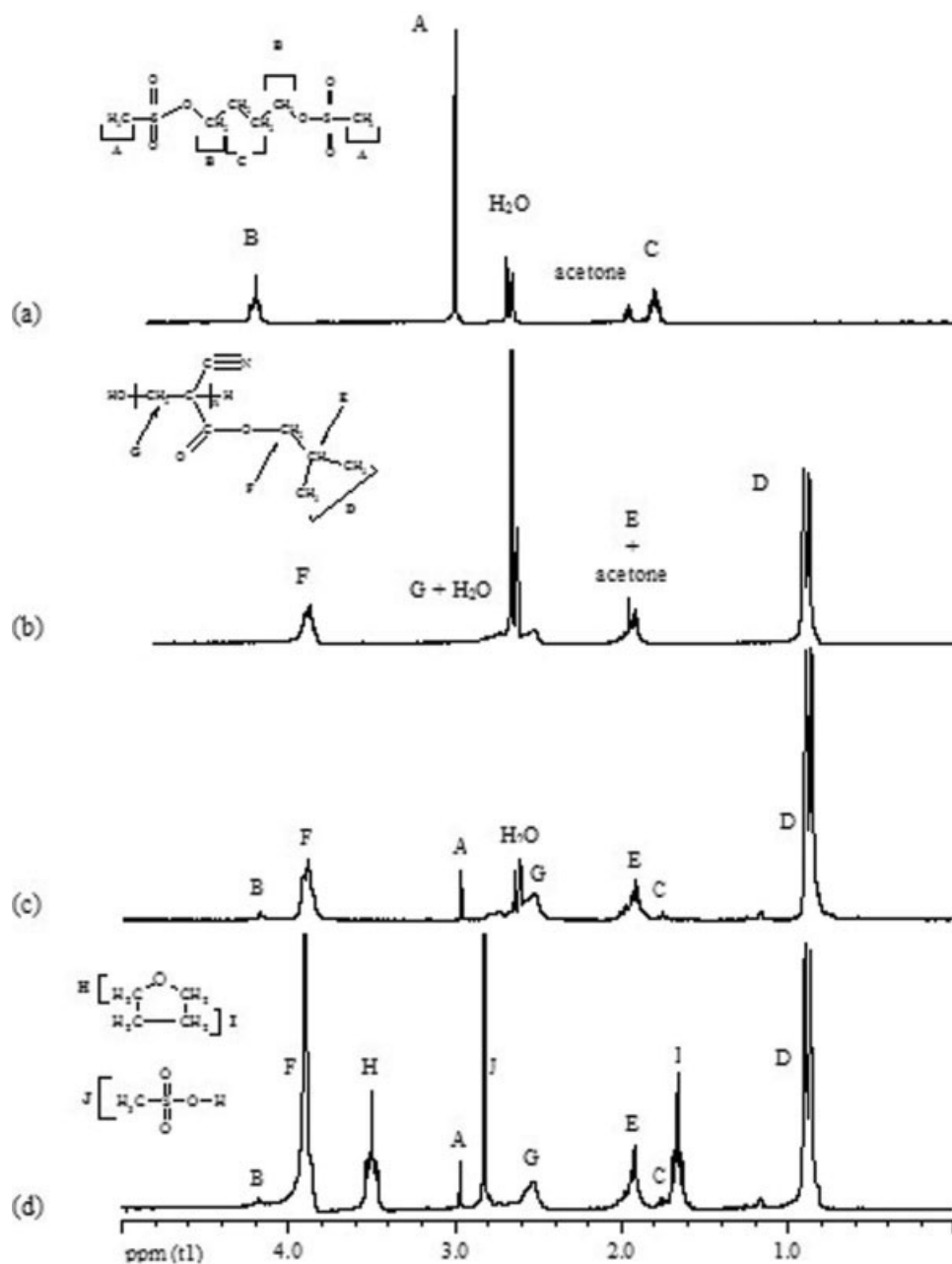


Figure 5. ^1H -NMR spectra in deuterated acetone (200 MHz). (a) busulfan, (b) PIBCA polymer, (c) busulfan-loaded nanoparticles (drug loading around 5.9% (w/w)), (d) busulfan-loaded nanoparticles doped with tetrahydrofuran and methanesulphonic acid.

Busulfan weight ratio (%) =

$$\frac{A_B/2 \times 256}{(A_B/2 \times 256) + (A_F/2 \times 153)} \times 100 \quad (3)$$

The weight ratio of busulfan present in the nanoparticles was found to be 6.5% (w/w), which is comparable to that determined using tritium-labelled drug ($5.9 \pm 0.2\%$ (w/w)) (Table III). These results also confirm that the entrapped drug was not degraded.

In Vitro Release Study. The *in vitro* release studies were performed in water or in rat plasma under sink condition,

using the PIBCA nanoparticle suspensions containing ($5.9 \pm 0.2\%$ (w/w) busulfan (Table III). After a rapid release during the first 10 min of 65% of the nanoparticle-associated busul-

TABLE IV. Features of Busulfan-Loaded Nanoparticles ^1H -Spectra: Peak Type (S, Singlet; D, Doublet; M, Multiplet), δ (Chemical Shift), Area (Integration of Peak)

Peak name	A	B	C	D	E	F	G
Peak type	S	M	M	D	M	M	M
δ (ppm)	2.9	4.1	1.7	0.9	1.9	3.9	2.5
Area	1	1	1	79	14	24	29

Peaks from A to G are reported in Fig. 5.

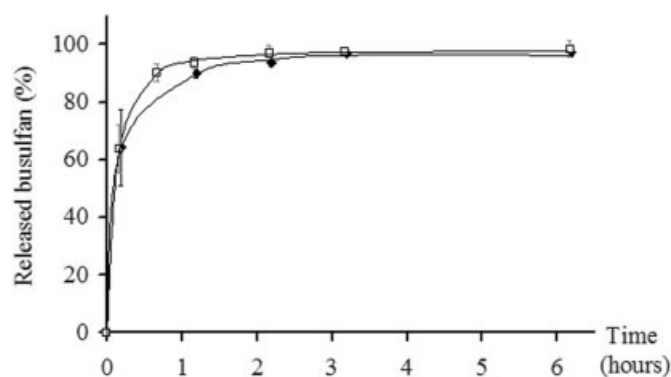


Figure 6. Busulfan release profiles from PIBCA nanoparticles at 37°C under sink conditions using water (◆) and rat plasma (□).

fan, the remaining drug was then released more slowly over 6 h (Figure 6). The drug adsorbed or located close to the nanoparticle surface was likely responsible for the observed quick release.

The octanol-water partition coefficient ($\log P_{ow}$) of busulfan was found to be -0.59 ,³¹ meaning that busulfan is a semi-polar drug with a partition coefficient in favor of water. Moreover, our previous studies by X-ray powder diffractometry showed that the methylsulfonate fragment of busulfan is nucleophilic (global charge of $-0.28 e$), whereas its carbon chain is electrophilic (global charge of $+0.56 e$).¹⁹ Yalkowsky et al.³² reported that the solubility of semipolar compounds in cosolvent–water mixtures were adequately described by a log-parabolic relationship. Indeed, the busulfan solubilization curve in ethanol–water mixtures was parabolic (data not shown). This indicates that busulfan is a semipolar drug, which may explain that upon dilution of the nanoparticle suspension with the release medium under sink condition, busulfan partitioned rapidly in favor of the dispersion medium, accounting for the immediate release.

CONCLUSION

We describe here for the first time the possibility to encapsulate large amounts of busulfan in nanoparticles, using a PIBCA polymer. Optimization studies enabled design of PIBCA nanoparticles displaying a drug loading close to 6% (w/w), together with a nanoparticle production yield of 71% (w/w). The chemical integrity of busulfan was preserved after loading into nanoparticles, as shown by ¹H-NMR studies. Molecular modeling suggested that there was specific dipole–dipole interaction between the methylsulfonate groups of busulfan and the nitrile groups of IBCA, which could explain the efficacy of PIBCA to encapsulate large amounts of busulfan. This shows the interesting input of molecular modeling in the drug delivery field.

The authors would like to acknowledge the French National Research Center (CNRS) and Ethypharm for their financial support, as well as Dr. K. Broadly from Loctite (Ireland) for his kindness in providing alkyl cyanoacrylate monomers.

REFERENCES

1. Clas SD. The importance of characterizing the crystal form of the drug substance during drug development. *Curr Opin Drug Discov Devel* 2003;6:550–560.
2. Nikolakakis I, Kachrimanis K, Malamataris S. Relations between crystallisation conditions and micromeritic properties of ibuprofen. *Int J Pharm* 2000;201:79–88.
3. Lin SY, Chen KS, Ten HH. Protective colloids and polylactic acid coaffecting the polymorphic crystal form and crystallinity of indomethacin encapsulated in microspheres. *J Microencapsul* 1999;16:769–776.
4. Alonso MJ. Nanoparticulate drug carrier technology. In: Bernstein H, editor. *Microparticulate System for the Delivery of Proteins and Vaccines*. New York: Marcel Dekker; 1995. p 203–242.
5. Brigger I, Chaminade P, Marsaud V, Appel M, Besnard M, Gurny R, Renoir M, Couvreur P. Tamoxifen encapsulation within polyethylene glycol-coated nanospheres. A new antiestrogen formulation. *Int J Pharm* 2001;214(1/2):37–42.
6. Dong Y, Feng S-S. Methoxy poly(ethylene glycol)-poly(lactide) (MPEG-PLA) nanoparticles for controlled delivery of anticancer drugs. *Biomaterials* 2004;25(14):2843–2849.
7. Peltonen L, Aitta J, Hyvönen S, Karjalainen M, Hirvonen J. Improved entrapment efficiency of hydrophilic drug substance during nanoprecipitation of poly(lactide) nanoparticles. *AAPS PharmSciTech* 2004;5:E16.
8. Dunn CD. The chemical and biological properties of busulfan (“Myleran”). *Exp Hematol* 1974;2:101–117.
9. Galton DAG. Myleran in chronic myeloid leukemia: Results of treatment. *Lancet* 1953;1:208–213.
10. Blazar BR, Ramsay NKC, Kersey JH, Krivit W, Arthur DC, Filipovich AH. Pretransplant conditioning with busulfan (Myleran) and cyclophosphamide for nonmalignant diseases. *Transplantation* 1985;39:597–603.
11. Hassan M, Öberg G, Bekassy AN, Aschan J, Ehrsson H, Ljungman P, Lönnnerholm G, Smedmyr B, Taube A, Wallin I, Simonsson B. Pharmacokinetics of high-dose busulfan in relation to age and chronopharmacology. *Cancer Chemother Pharmacol* 1991;28:130–134.
12. Grochow LB, Jones RJ, Brundrett RB, Braine HG, Chen TL, Saral R, Santos GW, Colvin OM. Pharmacokinetics of busulfan: Correlation with veino-occlusive disease in patients undergoing bone marrow transplantation. *Cancer Chemother Pharmacol* 1989;25:55–61.
13. Bhagwatwar HP, Phadungpojna S, Chow DSL, Andersson BS. Formulation and stability of busulfan for intravenous administration in high-dose chemotherapy. *Cancer Chemother Pharmacol* 1996;37:401–408.
14. Schuler US, Renner UD, Kroschinsky F, Johne C, Jenke A, Naumann R, Bornhäuser M, Deeg HJ, Ehninger G. Intravenous busulfan for conditioning before autologous or allogeneic human blood stem cell transplantation. *Br J Haematol* 2001;114:944–950.
15. Kennedy GLJ, Sherman H. Acute and subchronic toxicity of dimethylformamide and dimethylacetamide following various routes of administration. *Drug Chem Toxicol* 1986;9:147–170.
16. Yellowlees P, Greenfield C, McIntyre N. Dimethylsulphoxide-induced toxicity. *Lancet* 1980;2(8202):1004–1006.
17. Hassan Z, Nilsson C, Hassan M. Liposomal busulfan: Bioavailability and effect on bone marrow in mice. *Bone Marrow Transplant* 1998;22:913–918.
18. Bouligand J. Développement de nanosphères furtives de busulfan. Paris: Université Paris V; 2001.
19. Layre AM, Gref R, Richard J, Requier D, Chacun H, Appel M, Domb AJ, Couvreur P. Nanoencapsulation of a crystalline drug. *Int J Pharm* 2005;298:323–327.

20. Ghermani NE, Spasojevi-de Biré A, Bouhmaida N, Ouharzoune S, Bouligand J, Layre A, Gref R, Couvreur P. Molecular reactivity of busulfan through its experimental electrostatic properties in the solid state. *Pharm Res* 2004;21:598–607.
21. Fessi HC, Devissaguet JP. Process for the preparation of dispersible colloidal systems of a substance in the form of nanoparticles, US Patent 5,118,528, June 2, 1992.
22. Vauthier C, Couvreur P. Degradation of polycyanoacrylates. In: Steinbuechel A, editor. *Handbook of Biopolymers*. Weinheim: Wiley-VCH; 2002. p 457–490.
23. Urlaub E, Popp J, Roman VE, Kiefer W, Lankers M, Rosling G. Raman spectroscopic monitoring of the polymerization of cyanoacrylate. *Chem Phys Lett* 1998;298(1–3):177–182.
24. Eromosele IC, Pepper DC, Ryan B. Water effect on the zwitterionic polymerisation of cyanoacrylate. *Makromol Chem* 1989;190:1613–1622.
25. Kante B, Couvreur P, Dubois-Krack G, De Meester C, Guiot P, Roland M, Mercier M, Speiser P. Toxicity of polyalkylcyanoacrylate nanoparticles I: Free nanoparticles. *J Pharm Sci* 1982; 71:786–790.
26. Vauthier C, Dubernet C, Fattal E, Pinto-Alphandary H, Couvreur P. Poly(alkylcyanoacrylates) as biodegradable materials for biomedical applications. *Adv Drug Delivery Rev* 2003;55: 519–548.
27. Feit PW, Rastrup-Andersen N. 4-Methanesulfonyloxybutanol: Hydrolysis of busulfan. *J Pharm Sci* 1973;62:1007–1008.
28. Hassan M, Ehrsson H. Degradation of busulfan in aqueous solution. *J Pharm Biomed Anal* 1986;4:95–101.
29. Das SK, Tucker IG, Hill DJ, Ganguly N. Evaluation of poly-(isobutylcyanoacrylate) nanoparticles for mucoadhesive ocular drug delivery. I. Effect of formulation variables on physico-chemical characteristics of nanoparticles. *Pharm Res* 1995;12: 534–540.
30. Peracchia MT, Vauthier C, Puisieux F, Couvreur P. Development of sterically stabilized poly(isobutyl 2-cyanoacrylate) nanoparticles by chemical coupling of poly(ethylene glycol). *J Biomed Mater Res* 1997;34:317–326.
31. Westerhof GR, Ploemacher RE, Boudewijn A, Blokland I, Dillingh JH, McGown AT, Hadfield JA, Dawson MJ, Down JD. Comparison of different busulfan analogues for depletion of hematopoietic stem cells and promotion of donor-type chimerism in murine bone marrow transplant recipients. *Cancer Res* 2000;60(19):5470–5478.
32. Yalkowsky SH, Roseman TJ. Solubilization of drugs by cosolvents. In: Yalkowsky SH, editor. *Techniques of Solubilization of Drugs*. New York: Marcel Dekker; 1980. p 91–135.